Available online at www.sciencedirect.com
SCIENCE DIRECT
Catalysis Today 107–108 (2005) 520–530
CATALYSIS TODAY
www.elsevier.com/locate/cattod

# Deep HDS on doped molybdenum carbides: From probe molecules to real feedstocks

Patrick Da Costa *, Jean-Marie Manoli, Claude Potvin, Gérald Djéga-Mariadassou

*Laboratoire Réactivité de Surface, CNRS UMR 7609, Université Pierre et Marie Curie, 4 Place Jussieu, Case 178, Tour 54-55, 75252 Paris Cedex 05, France*

Available online 31 August 2005

**Abstract**

Deep HDS on phosphorus and nickel–alumina-supported molybdenum oxycarbides was studied, first, with probe molecules then with real feedstocks. Catalysts were characterized by elemental analysis, X-ray diffraction, CO chemisorption, transmission electron microscopy, X-ray photoelectron spectroscopy and infrared spectroscopy. Propene and tetralin hydrogenation were used to probe the activity of the doped materials. Hydrodesulfurization of 4,6-dimethyldibenzothiophene was investigated as a probe for the deep HDS of diesel fuel. For contact times ranging from 0 to 0.4 s, the HDS of 4,6-DMDBT is zeroth-order with respect to the reactant and proceeds via two parallel routes, direct desulfurization and hydrogenation pathways, the former being preponderant. Phosphorus and nickel modify the catalytic behaviour and induce the highest HDS activity. Deep hydrodesulphurization (HDS) of diesel fuels was carried out on promoted or non-promoted $Mo_2C$-supported $\gamma$-$Al_2O_3$ and on bulk $Mo_2C$ under standard industrial conditions. The effect of the promoter was investigated for different feedstocks on HDS and hydrogenation (HDA) with very low levels of sulfur. The HDS conversion indicated that P-doped alumina supported carbide catalysts were as active as a commercial Co–Mo/$Al_2O_3$ catalyst for low level of sulfur in the feed. Furthermore, the refractory compounds, such as 4,6-DMDBT were only transformed on molybdenum carbide catalyst under industrial conditions for hydrotreated gas oils. For feeds containing less than 50 wt. ppm in sulfur, P-doped carbides were more active than commercial catalysts for HDA, as well as deep HDS or HDN.


*Keywords:* Molydenum carbide; Phosphorus; Deep HDS; 4,6-DMDBT; Gas oil

## 1. Introduction

The future specification more and more drastic for sulfur-containing diesel fuels (sulfur content as low as 50 wt. ppm by the year 2005 in Europe) is leading refiners to develop novel catalysts for deep desulfurization. To satisfy these demands for high-purity products, it is important to remove alkyl-substituted aromatic sulfur compounds. It is now well established that 4,6-dimethyldibenzothiophene (4,6-DMD BT) with alkyl groups near the sulfur atom is one of the most refractory [1–3]. Numerous studies recently reviewed [4,5] have been carried out in the last few years to better understand why such species are the most difficult to eliminate. Conventional sulfided Co(Ni)Mo/Al catalysts have been much improved for hydrodesulfurization (HDS) in the last decades but there is not a recognized alternative to these materials yet. Only few studies with transition metal carbides deal with deep HDS, using model refractory compounds, such as 4,6-DMDBT [6–8] or industrial conditions [9–11]. The aim of the present work is to present the activity of bulk extrudates of molybdenum carbides and alumina-supported molybdenum-based carbides, promoted with phosphorus (phosphorus being introduced as heteropolyanions with defined P/Mo ratio) or nickel, for deep HDS, at very low level of sulfur, with probe molecules in laboratory scale conditions and with real feedstocks under industrial conditions in a three-phase flow reactor. These materials were compared to industrial hydrotreating catalysts.

* Corresponding author. Tel.: +33 1 44 27 36 26; fax: +33 1 44 27 60 33.
*E-mail address:* dacosta@ccr.jussieu.fr (P. Da Costa).

0920-5861/$ – see front matter © 2005 Elsevier B.V. All rights reserved.
doi:10.1016/j.cattod.2005.07.166

## 2. Experimental

### 2.1. Catalyst preparation

The used precursors are presented in Table 1. For non-promoted catalysts, commercial ammonium heptamolybdate $(NH_4)_6Mo_7O_{24}{\cdot}xH_2O$ (Acros) was used as precursor. For phosphorus-promoted catalysts, commercial $H_3PMo_{12}O_{40}{\cdot}xH_2O$ (Acros) and precursors synthesized in the laboratory [8], such as $(NH_4)_6P_2Mo_{18}O_{62}{\cdot}xH_2O$ and $(NH_4)_6P_2Mo_5O_{23}{\cdot}xH_2O$, were used. Impregnated nickel-promoted catalysts (HR346C), were supplied by Procatalyse. The support consisted of γ-alumina provided by Procatalyse. Supported molybdenum (Mo, 10 wt.%) materials were prepared using the incipient wetness method. The impregnated samples were dried at 393 K for 12 h. Bulk and supported carbides were prepared by temperature-programmed reaction (TPR), using a modification of the procedure described elsewhere [12]. First, the extrudates were heated in flowing argon (flow rate, 60 $cm^3\ min^{-1}$) and held at 673 K for 8 h. Then, the materials were carburized by a temperature programmed reaction (TPR) in flowing $CH_4/H_2$ (60 $cm^3\ min^{-1}$), the temperature being raised linearly from 673 to 950 K. At this final temperature, the $CH_4/H_2$ flow was switched to hydrogen and the system was cooled rapidly to room temperature (RT). After cooling to RT, the hydrogen flow was switched to $O_2$/Ar mixture (1% (v/v)) for passivation step (1 h) before characterization or catalysis experiments. Extrudates of bulk or supported carbides were crushed and sieved between 0.25 and 0.4 mm. The powders were used for characterization and catalytic tests with probe molecules. For sake of comparison, commercial catalysts (HR346C-Procatalyse) and nickel precursors were also used. The prepared catalysts are presented in Table 1.

### 2.2. Characterization of catalysts

Before and after reaction, the passivated catalysts were characterized by XRD, CO chemisorption, TEM and EDS analysis.

Powder X-ray diffraction (XRD) was carried out in a Siemens model D-500 diffractometer using the Cu Kα radiation.

The selective chemisorption of CO was used to evaluate active metal sites before catalytic test and was performed by a pulse technique at 293 K. Hence, the CO consumption could be determined and the amount of CO chemisorbed by the sample deduced. Prior to chemisorption, the passivated carbide catalysts were reduced in flowing $H_2$ (12 $cm^3\ min^{-1}$) at 773 K for 4 h.

High-resolution transmission electron microscopy (HRTEM) was performed to determine the particle size of molybdenum carbides supported on alumina and to check the dispersion of the supported carbides. HRTEM studies were performed on a JEOLJEM 100 CXII apparatus associated with a top entry device and operating at 100 kV. Energy dispersive spectroscopy (EDS) analysis (STEM mode) was performed with the same apparatus using a LINK AN 10000 system, connected to a silicon–lithium diode detector, and multichannel analyser. The EDS analyses were obtained from large domains of samples (150 nm × 200 nm to 400 nm × 533 nm).

X-ray photoelectron spectra were recorded with a VG Scientific, Escalab 200R spectrometer equipped with Mg Kα X-ray source and a hemispherical analyzer. In the case of Ni-containing compounds, an Al Kα source was used. Sealed glass tubes containing the materials were opened in a glove box (dry argon) and introduced into the spectrometer chamber without exposure to air. The vacuum during the measurements was typically less than $5 \times 10^{-6}$ Pa and the scan speed 0.02 eV/s with 0.1 eV $step^{-1}$. The Al 2p line of $Al_2O_3$ at 74.0 eV was taken as reference to calculate binding energies and account for the charging effect. Experimental peaks were decomposed into components using mixed Gaussian–Lorentzian functions and a non-linear least-squares fitting algorithm; Shirley background subtraction was applied. An intensity ratio of 2/3 and a splitting of 3.2 eV were used to fit the Mo 3d peaks. The surface composition (in at.%) of samples was determined from the integrated peaks of C 1s, O 1s, Mo 3d, P 2p and Ni 2p using their respective experimental sensitivity factors.

The passivated catalyst powders were pressed into self-supported wafers (ca. 5 mg $cm^{-2}$, dia. = 1.6 cm) and re-treated in situ in the IR cell. The system was pumped down to $10^{-2}$ Pa, the temperature raised from RT to 773 K at 4 K $min^{-1}$ and held at 773 K for 30 min. Three cycles of

Table 1
Catalysts, precursors, pH of impregnation solutions

| Catalyst | Precursor | pH | Source | Treatment |
|---|---|---|---|---|
| $Mo_2C/Al$ | $(NH_4)_6H_2Mo_7O_{24}{\cdot}xH_2O$ | 3.9 | Acros | I/C |
| $Mo_2CP(0.08)/Al$ | $H_3PMo_{12}O_{40}{\cdot}xH_2O$ | 1.2 | Acros | I/C |
| $Mo_2CP(0.11)/Al$ | $(NH_4)_6P_2Mo_{18}O_{62}{\cdot}xH_2O$ | 3.9 | Home-made[a] | I/C |
| $Mo_2CP(0.40)/Al$ | $(NH_4)_6P_2Mo_5O_{23}{\cdot}xH_2O$ | 4.2 | Home-made[a] | I/C |
| $NiMo_2C/Al$ | – | – | Procatalyse | C |
| NiC/Al | $Ni(NO_3)_2{\cdot}6H_2O$ | 3.8 | Fluka | I/C |
| Ni/Al | $Ni(NO_3)_2{\cdot}6H_2O$ | 3.8 | Fluka | I/R |

I, impregnated; C, carburized; R, reduced.
[a] Synthesis from Ref. [8].

hydrogen reduction ($P_{H_2}$ = 2.7 × $10^4$ Pa, contact time = 1, 2 and 1 h) at 773 K followed by evacuation at the same temperature were performed, the last evacuation being prolonged until the residual pressure in the cell reached 3 × $10^{-2}$ Pa. The activated catalysts were exposed to pyridine (267 Pa) at RT and evacuated at 473 K or RT. In an additional experiment, the activated catalyst was treated with $H_2O$ (133 Pa) at RT. The IR spectra were recorded at RT using a Nicolet 60SX FT-IR spectrometer. For sake of comparison, spectra and band area values presented in this work were normalized to a disk of 5 mg $cm^{-2}$.

Chemical analysis by atomic emission spectrometry or by atomic absorption was performed at the ''Service Central d'Analyses du CNRS'' in order to determine the Mo, P and C contents for both the fresh and spent catalysts.

### 2.3. High pressure probe reactions

Tetralin hydrogenation was chosen as model reaction for the hydrogenation of aromatics in diesel fuels. The reaction was carried out at 573 K, at a total pressure of 4 MPa. Tetralin was diluted in *n*-heptane. Partial pressures of tetralin, *n*-heptane and hydrogen were 0.01, 0.93 and 3.06 MPa, respectively. The liquid products were collected every hour and analysed by gas chromatography (VARIAN) using a flame ionization detector (FID) and a capillary column (DB1, J&W Scientific). Before reaction, the supported carbides (0.2 g) were pretreated in situ, at 423 K and 4 MPa in flowing hydrogen (1 L $h^{-1}$) to remove the passivation layer.

Hydrodesulfurization of 4,6-DMDBT was chosen as model reaction for the HDS of diesel fuels. The reaction was carried out at 613 K and a total pressure of 4 MPa; the 4,6-DMDBT was diluted in decalin. Under standard conditions, the partial pressures were: 4,6-DMDBT, 0.001 MPa; decalin, 0.888 MPa; hydrogen, 3.111 MPa. The ratio of $H_2$/liquid feed flow was set to 500. Before reaction, the supported carbides (0.4 g) were pretreated in situ, at 423 K and 4 MPa in flowing hydrogen (100 $cm^3$ $min^{-1}$) for 1 h. Then the feedstock was introduced and the temperature raised to 613 K. The liquid products were periodically collected and analyzed by gas chromatography. All quantitative chromatographic analyses were performed by using an external standard namely 1-methylnaphthalene.

The partial pressure of $H_2S$ depended on the HDS conversion and ranged from 0 to 0.0009 MPa, which corresponded to 90% conversion of 4,6-DMDBT.

### 2.4. Real feedstock reactions

HDS experiments with gas oil feedstocks were carried out in a continuous flow microreactor. The catalyst bed consisted of 30 $cm^3$ (extrudates, 20 g), which was diluted with SiC to fulfill the plug flow conditions required. Two gas oils (TOTAL) were used as representative feed for second-stage of deep HDS processing. The sulfur content of gas oils was: 520 wt. ppm S and 135 wt. ppm for GO1 and GO2, respectively. The catalysts were pretreated in situ at 423 K, under similar conditions to those of model feed experiments presented elsewhere [8]. The catalysts were tested at 613 K with WHSV = 2.6 goil $g^{-1}$ cat $h^{-1}$ and a constant total pressure of 3.0 MPa. The $H_2$/HC was 500 N $cm^3/cm^3$. No additional $H_2S$ was added to the feed. The product samples were collected and analyzed off-line, using a Hewlett-Packard (HP5890 series) gas chromatograph (GC) equipped with a 50 m capillary fused silica column (PONA) associated with a sulfur specific detector (Sievers, MODEL SCD 355 B). Quantitative analysis of the sulfur concentration was determined by energy X-ray fluorescence (XRF) spectroscopy with a X-MET 920 (Metorex) sulfur analyzer. Aromatic transformation experiments with deep hydrotreated gas oil feedstocks were carried out in the same continuous flow microreactor to check the hydrogenation properties of the catalysts. The operating conditions consisted in using a catalyst bed ranging from 10 to 20 g, diluted with SiC. The catalytic experiments were performed at 613 K, with WHSV = 1.0 goil $g^{-1}$ cat $h^{-1}$ and a constant total pressure of 3.0 MPa. The $H_2$/HC ratio was 500 N $cm^3/cm^3$. Two gas oils were used with 0.5 wt. ppm S (GO3) and 47 wt. ppm S (GO4) determined by XRF. Aromatic distribution (mono-, di-, polycyclic compounds) of the gas oil, was deduced from Ultraviolet spectrometry using the Burdett method [13]. The aromatic conversion was calculated, using the normalised European standards (CEN) by high pressure liquid chromatography (HPLC).

## 3. Results and discussion

### 3.1. Physical and chemical characterizations

TEM and EDS measurements were performed to estimate the particle size of molybdenum carbides. TEM showed no particles on $Mo_2C$/Al or alumina-supported carbides promoted by nickel. For all the catalysts, the molybdenum content estimated by EDS did not change whatever the area analyzed, which indicated that the molybdenum was homogeneously dispersed on the support. The phosphorus was also well dispersed and the P/Mo ratios were close to those in the heteropolyanion structure, on the scale of the domains examined (Table 2). Moreover, EDS analysis showed that after carburization, the results were the same. X-Ray diffraction (XRD) led to the same conclusions (Fig. 1). For alumina-supported molybdenum (10 wt.% Mo) carbide, particles were not detected by XRD, which means that the particles of $Mo_2C$ were well dispersed on the support. Furthermore, the presence of phosphorus and nickel did not affect these conclusions (Fig. 1).

The selective chemisorption of CO was used to titrate the number of active metal sites on alumina-supported molybdenum carbides. The CO chemisorption was performed by a

Table 2
EDS analysis of alumina supported based carbides

| Catalyst | Mo/Al | P/Mo theoritical | P/Mo analysed after synthesis | P/Mo analysed after carburization | Ni/Al theoritical | Ni/Al analysed |
|---|---|---|---|---|---|---|
| $Mo_2C$/Al | 0.070 | 0 | | | | |
| $Mo_2CP(0.08)$/Al | 0.068 | 0.08 | 0.08 | 0.08 | | |
| $Mo_2CP(0.11)$/Al | 0.069 | 0.11 | 0.12 | 0.11 | | |
| $Mo_2CP(0.40)$/Al | 0.067 | 0.40 | 0.42 | 0.41 | | |
| $NiMo_2C$/Al | 0.065 | | | | 0.26 | 0.27 |
| NiC/Al | | | | | 0.26 | 0.25 |
| Ni/Al | | | | | 0.26 | 0.27 |

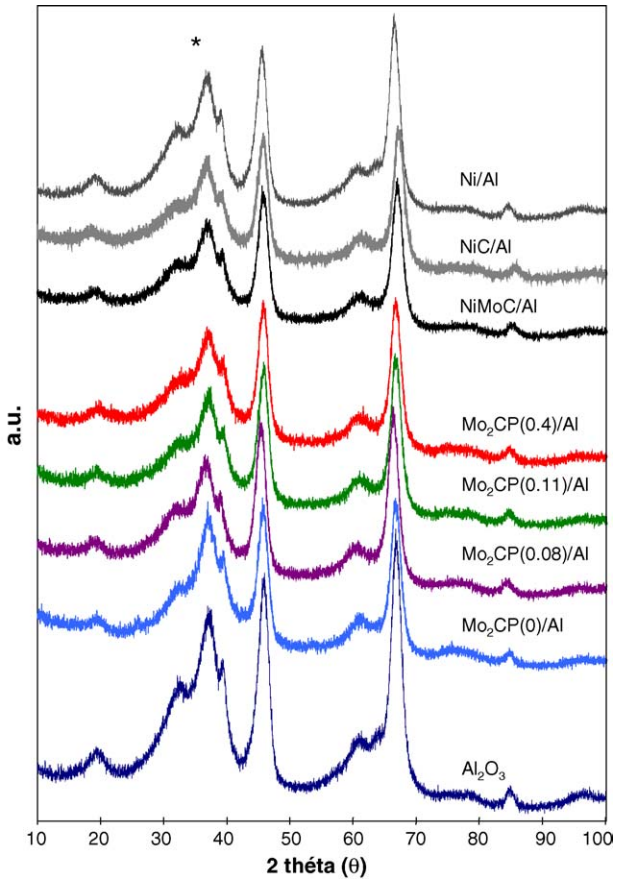


Fig. 1. XRD patterns of alumina-supported molybdenum-based carbides (*:β-Mo2C (JCPDS 35-787)).

pulse technique at 293 K [14,15]. As shown in Table 3, the CO uptakes of the samples examined range from 26 to 45 μmol $g^{-1}$. For the supported molybdenum carbides, the values were smaller than those reported [14–16]. The material synthesized with P/Mo = 0.4 precursor had a lower CO uptake (26 μmol $g^{-1}$) than the catalyst without any additive. No correlation could be observed between P content and CO uptake, neither between the different promoters and CO uptake.

For the Ni-promoted catalyst $NiMo_2C$/Al, the chemisorption capacity was slightly higher than that measured on $Mo_2C$/Al. This result was in agreement with the literature [14].

Propene hydrogenation (a structure-insensitive reaction) was selected to evaluate the role of phosphorus on the activity of our materials at atmospheric pressure. The reaction was carried out in a flow reactor at 250 K. The gas mixture (the $H_2/C_3H_6$ molar ratio was fixed at 6.7 and the total flow rate at 117 $cm^3$ $min^{-1}$) was fed into a Pyrex reactor loaded with 0.1 g of catalyst on a sintered glass disk (dia., 1 cm). The only product observed was propane. Prior to each run, passivated catalysts were pretreated in situ at 773 K in flowing $H_2$ (12 $cm^3$ $min^{-1}$) for 4 h. As reported in Table 3, the P-containing catalysts had higher hydrogenation activity, as indicated by the values of the initial conversion at 250 K. As already noted for bulk catalysts [17], the presence of phosphorus was closely related to the hydrogenation character of the molybdenum carbides.

The Ni-based or Ni-promoted alumina-supported catalysts had better hydrogenation properties than the P-promoted carbide ones with initial conversions of 78–

Table 3
CO chemisorption, $S_g$ measurements and activity in hydrogenation with probe molecules (propene at 250 K and tetralin at 573 K)

| Catalyst | $S_g$ ($m^2$ $g^{-1}$) | Chemisorbed CO (μmol $g^{-1}$) | Initial propene conversion (%) | Steady-state tetralin conversion (%) |
|---|---|---|---|---|
| Alumina | 191 | 0 | 0 | 0 |
| $Mo_2C$/Al | 171 | 40 | 3.0 | 7 |
| $Mo_2CP(0.08)$/Al | 168 | 45 | 6.1 | 16 |
| $Mo_2CP(0.11)$/Al | 167 | 41 | 16.1 | 13 |
| $Mo_2CP(0.40)$/Al | 168 | 26 | 19.8 | 15 |
| $NiMo_2C$/Al | 165 | 44 | 77.9 | 17 |
| NiC/Al | 178 | – | 82.7 | – |
| Ni/Al | 180 | – | 94.1 | – |

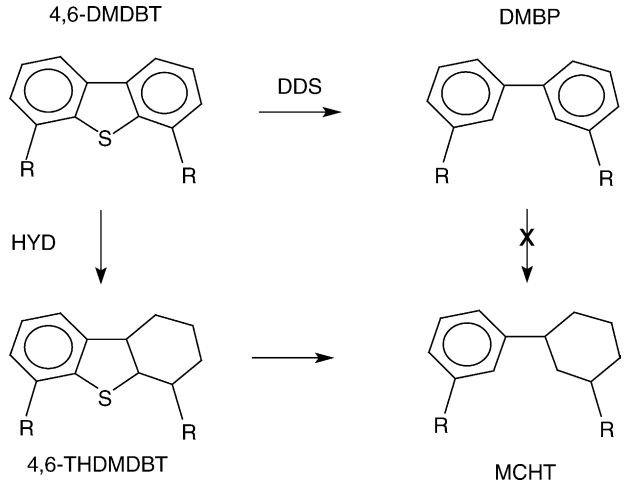


Fig. 2. Pathways of HDS of 4,6-DMDBT.

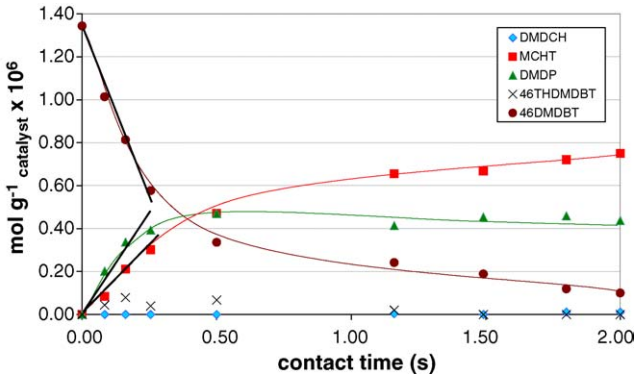


Fig. 3. Hydrodesulfurization of 4,6-DMDBT over alumina supported molybdenum based catalyst: moles of reactant and products per gram of catalyst vs. contact time on $Mo_2CP(0.4)/Al$.

94% and 6–20%, respectively. The initial conversions of NiC/Al and $NiMo_2C/Al$ were comparable but these carburized catalysts were rapidly deactivated, contrary to Ni/Al. The catalysts were also tested in tetralin hydrogenation at high pressure. Activities were enhanced by phosphorus and Ni addition (Table 3).

### 3.2. Reactivity of promoted alumina-supported molybdenum carbides in 4,6-DMDBT HDS

#### 3.2.1. Phosphorus promoted catalysts

It is well known that the HDS of 4,6-DMDBT on sulfided alumina-supported molybdenum oxides leads to methylcyclohexyltoluene (MCHT) and dimethylbiphenyl (DMBP) [18], via two parallel pathways, HYD and DDS (Fig. 2). With $Mo_2C/Al$, we showed [7] that the HDS products, DMBP and MCHT, were independent for conversions lower than 45%. In fact, DMBP was never hydrogenated to MCHT in the HDS reaction [7]. The Fig. 3 presents the kinetics study for $Mo_2CP(0.4)/Al$ catalyst. We proposed a mechanism for carbide catalysts in agreement with that of sulfided catalysts [18]. Kinetic studies of 4,6-DMDBT hydrodesulfurization [7] showed that two domains existed depending on the contact time for alumina-supported molybdenum carbide ($Mo_2C/Al$). At low contact time (i.e. conversion lower than 45%), an overall zeroth order was found for the reaction. The adsorbed 4,6-DMDBT [$DMDBT^*$], saturated the surface. It was assumed to be the most abundant surface intermediate (MASI) [Ref. 42 in 7]; the other species being neglected. Then [$DMDBT^*$] was equal to the total number of sites [L]. In this case, the expression of the overall reaction rate HDS was the sum (Eqs. (1) and (2)) of the DDS ($r_{DDS}$) and HYD ($r_{HYD}$) rates.

$$r_{HDS} = (k_{1H,H_2} + k_{1D})[DBDBT^*] = k_1[L] \quad (1)$$

$$r_{HDS} = r_{HYD} + r_{DDS} = k_1[L] \quad (2)$$

In which, $k_{1H,\ H2}$ was the first rate constant of the HYD route and $k_{1D}$ the rate constant of the first elementary step in the direct DDS route, according to Eq. (2).

The rates of MCHT ($r_{HYD}$) and DMBP ($r_{DDS}$) formation, expressed in mole of products per gram of catalyst, were calculated at low contact time (<0.4 s). Two zones were observed for all catalysts (Fig. 3). The kinetic results are presented in Table 4. The HDS rate increased with the phosphorus content, if we consider the same type of non-acidic precursors. The HDS rate increased from $1.87 \times 10^{-6}$ mol $g^{-1}$ $s^{-1}$ for $Mo_2C/Al$ to $3.31 \times 10^{-6}$ mol $g^{-1}$ $s^{-1}$ for $Mo_2CP(0.40)/Al$. The selectivity ratio of the reaction, defined as the rate ratio $r_{HYD}/r_{DDS}$, ranged from 0.4 to 0.7. Then, the phosphorus promotion led to an enhancement of the overall HDS. The catalyst, $Mo_2CP(0.08)/Al$, derived from the Keggin-type heteropolyacid, $H_3PMo_{12}O_{40}$, was more efficient than the others phosphorus-promoted materials. The P content was lower but the increase of the rate was very important. For this catalyst, the HDS rate was $3.81 \times 10^{-6}$ mol $g^{-1}$ $s^{-1}$ and the selectivity 0.4. In

Table 4
Rate and selectivity ratio in HDS of 4,6-DMDBT on alumina-supported molybdenum carbides: effect of P, Ni

| Catalyst | $r_{HDS}$ ($10^6 \times$ mol $g^{-1}$ $s^{-1}$) | $r_{HYD}$ ($10^6 \times$ mol $g^{-1}$ $s^{-1}$) | $r_{DDS}$ ($10^6 \times$ mol $g^{-1}$ $s^{-1}$) | $r_{HYD}/r_{DDS}$ |
|---|---|---|---|---|
| $Mo_2C/Al$ | 1.87 | 0.76 | 1.10 | 0.7 |
| $Mo_2CP(0.08)/Al$ | 3.81 | 1.14 | 2.74 | 0.4 |
| $Mo_2CP(0.11)/Al$ | 2.50 | 0.86 | 1.58 | 0.5 |
| $Mo_2CP(0.40)/Al$ | 3.31 | 1.25 | 1.83 | 0.7 |
| $NiMo_2C/Al$ | 4.10 | 1.03 | 3.11 | 0.3 |

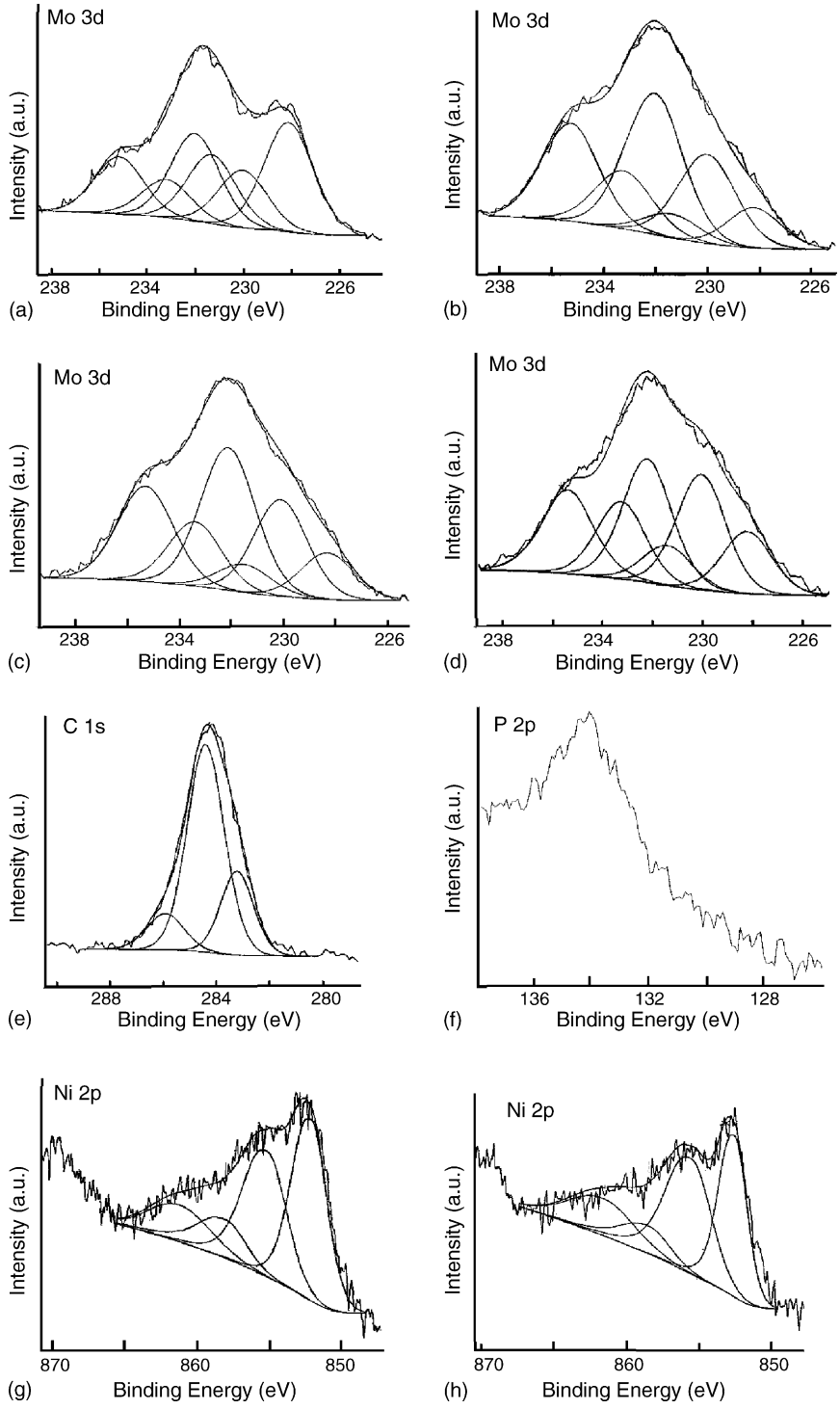


Fig. 4. Superposition of experimental XPS spectra and spectra after decomposition for P-doped alumina-supported molybdenum carbides and Ni-doped molybdenum carbides: Mo 3d (inset) level: (a) P/Mo = 0; (b) P/Mo = 0.08; (c) P/Mo = 0.11; (d) P/Mo = 0.4. C 1s level: (e) P/Mo = 0.4. P 2p level: (f) P/Mo = 0.4. Ni 2p level: (g) NiC/Al; (h) $NiMo_2C$/Al.

this case, the DDS rate was higher than in other P-doped alumina-supported molybdenum carbides. The support acidity of this catalyst has been probably modified during the impregnation process, leading to a more acidic catalyst.

### 3.2.2. *Nickel promoted catalysts*

The HDS of 4,6-DMDBT was also studied on $NiMo_2C$/Al. The catalyst showed the same behaviour as for $Mo_2CP$/Al. Once again, two kinetic domains and the same reaction products (DMBP and MCHT) were observed. The overall

HDS rate ($4.10 \times 10^{-6}$ mol $g^{-1}$ $s^{-1}$) was twice that of $Mo_2CP/Al$ ($1.87 \times 10^{-6}$ mol $g^{-1}$ $s^{-1}$). The selectivity ratio of $NiMo_2C/Al$ was lower than $Mo_2CP(X)/Al$ catalysts. The HYD rate was slightly enhanced but the DDS rate was three times higher than the $Mo_2C/Al$ material. For sake of comparison, we carried out 4,6-DMDBT HDS with alumina-supported carburized nickel NiC/Al. In this case, a lower activity was observed and the material deactivated in less than 1 h. Alumina-supported nickel catalyst Ni/Al, was rapidly sulfided under the reaction conditions and was not active after 2 h on stream. Therefore, nickel addition enhanced HDS conversion, particularly by the DDS route, confirming that there is a synergetic effect of nickel in alumina-supported $NiMo_2C/Al$.

### 3.3. Active site identification by FT-IR and XPS, correlation with HDS activity

#### 3.3.1. Non-promoted catalysts

The distribution of Mo oxidation states for molybdenum oxycarbide was estimated by decomposition of the Mo 3d spectra using X-ray photoelectron spectroscopy (Fig. 4).

Curve-fitting of Mo 3d peaks was accomplished using linked doublets (Mo $3d^{5/2}$–Mo $3d^{3/2}$) corresponding to three different molybdenum species with binding energies lower than 232.4 eV and higher than 228.0 eV. The XPS results for P-doped materials are summarized in Table 5. A characteristic species with a Mo $3d^{5/2}$ binding energy lower than 229 eV was identified. This binding energy found around 228.2 eV can be attributed to a carbide phase close to molybdenum in a zerovalent state, which is generally found at 227.9 eV in bulk molybdenum carbides. It has been denoted as $Mo^{\delta+}$ and is assumed to be involved in a Mo–C bond. For non-doped alumina-supported molybdenum carbide, 42% of the molybdenum was present in the $Mo^0$ or $Mo^{\delta+}$ state.

#### 3.3.2. P- or Ni-promoted catalysts

On the contrary, values for P- and Ni-doped catalysts were 13–20% and 32%, respectively. The abundance of this $Mo^{\delta+}$ peak, which is characteristic of a metal-like site, was lower for P- and Ni-containing carbides. However, the hydrogenation and HDS properties were enhanced in the presence of P and Ni. This suggests that while this metal-like species is important for the HDS reactions, an oxycarbide phase which corresponds to a higher oxidation state of molybdenum in the alumina-supported carbides is also required. This molybdenum oxidation state is close to 4+ and to a binding energy of 230.0 eV. The area of the oxycarbide peaks ranged from 34–38% for P/Mo ratios ranging from 0.08–0.40, whereas for $Mo_2C/Al$, it was only 23% of the total molybdenum area. Similarly, the increase in the oxycarbide phase and, consequently, in the activity can explain the higher activity of P-containing supported materials in HDS reactions.

For the Ni-containing catalyst, the abundance of $Mo^{\delta+}$ was lower than for $Mo_2C/Al$ but higher than for $Mo_2CP(X)/Al$ (with X = P/Mo) carbides. Moreover, the area of the molybdenum peak involved in the oxycarbide phase ($Mo^{4+}$) was only 25% of the total molybdenum peak area, which was close to the values found for $Mo_2C/Al$. The proportion of various species for $Mo_2C/Al$ and $NiMo_2C/Al$ were more similar than for the corresponding P-containing catalysts.

For all the alumina-supported molybdenum carbides, the C 1s signal was also decomposed. Three components were found, the lowest binding energy was attributed to carbon from the carbide phase (283.1–283.5 eV); the second component (around 284.5 eV) was related to contamination carbon; finally at higher binding energy (285.9–286.4 eV), the third component, was assigned to oxidized carbon entities (C–O). The relative area of the carbon peaks involved in the C–O bond can be ranked in the same sequence in terms of reactivity as in the HDS of 4,6-DMDBT, where the overall rate was found to rise as follows: $Mo_2C < Mo_2CP(0.11) < Mo_2CP(0.40) < Mo_2CP(0.08)$. Therefore, we can assume that activity is related to the area of $Mo^{4+}$ peak (oxycarbide species) for alumina-supported molybdenum carbides.

To further characterize the acidic sites of supported carbide catalysts, pyridine was used as probe molecule. Pyridine can coordinate with Lewis acid sites while it is protonated by sufficiently acidic sites. On alumina-supported molybdenum carbide catalysts, the adsorption of pyridine followed by evacuation at 473 K gave several bands at about 1622, 1608 (sh), 1577, 1494 and 1452 $cm^{-1}$ (Fig. 5). These bands are characteristic of Lewis acid sites [19]. No peak corresponding to Brønsted acid sites (1540 cm) was observed [8]. In the 1625–1600 $cm^{-1}$ region, two bands (at 1622 and 1608 $cm^{-1}$) indicated Lewis acid sites of strong and medium acid strength, respectively.

Table 5
XPS results for alumina-supported molybdenum carbides with different P/Mo ratios; comparison with non-doped material

| Catalyst | C 1s | | | Mo $3d_{5/2}$ | | |
|---|---|---|---|---|---|---|
| | Carbide | | Oxicarbide | $Mo^{\delta+}$ carbide | $Mo^{4+}$ oxycarbide | $Mo^{6+}$ oxide |
| $Mo_2C/Al$ | 283.2 (23%) | 284.4 (65%) | 285.9 (12%) | 228.1 (42%) | 230.0 (23%) | 232.0 (35%) |
| $Mo_2CP(0.08)/Al$ | 283.5 (11%) | 284.8 (53%) | 286.4 (36%) | 228.2 (13%) | 230.0 (34%) | 232.0 (53%) |
| $Mo_2CP(0.11)/Al$ | 283.1 (37%) | 284.4 (51%) | 285.9 (12%) | 228.3 (15%) | 230.1 (34%) | 232.1 (51%) |
| $Mo_2CP(0.40)/Al$ | 283.2 (28%) | 284.4 (49%) | 285.9 (23%) | 228.2 (20%) | 230.0 (38%) | 232.2 (42%) |
| $NiMo_2C/Al$ | | | | 228.2 (32%) | 230.0 (25%) | 232.3 (43%) |

Binding energies (eV) and concentrations (%) of C 1s, Mo $3d_{5/2}$ species.

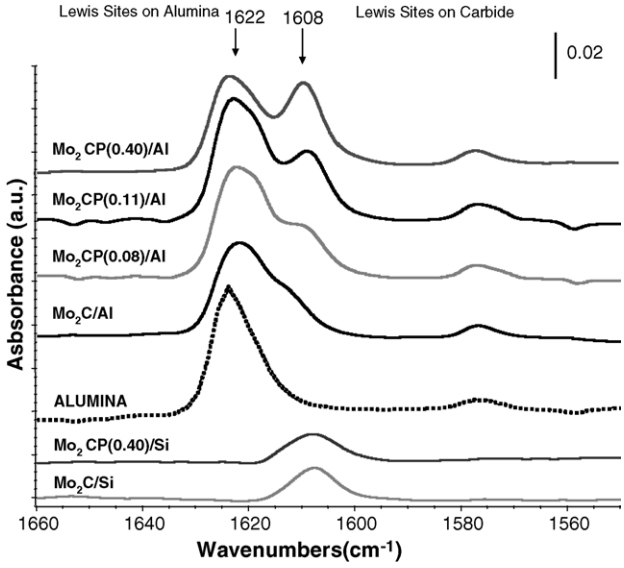


Fig. 5. IR spectra of species resulting from pyridine evacuation at 473 K on various P-doped alumina-supported molybdenum carbides: comparison with silica-supported and Ni-doped alumina-supported molybdenum carbides.

Comparison with pure alumina showed that the peak at 1622 $cm^{-1}$ can be attributed to pyridine coordinated on unsaturated surface $Al^{3+}$ sites of the support [20] while that at 1608 $cm^{-1}$ could be attributed to the supported carbide phase. When pyridine was adsorbed at 473 K on silica-supported carbide catalyst, only the peak at 1608 $cm^{-1}$ was detected. This confirms that there are weak Lewis acid sites located on the oxygen-modified carbide, as detected by CO [8]. Comparison with previous results showed that Lewis acid sites were stronger on the oxygen-modified molybdenum carbide ($\nu \sim 1608\ cm^{-1}$) than on the molybdenum sulfide ($\nu \sim 1600\ cm^{-1}$).

The intensity of the acid sites band (1608 $cm^{-1}$) increased with the amount of P in P-doped carbide catalysts supported on alumina (Fig. 5). No Brønsted acidic sites were detected. Thus, increase of the number of Lewis sites in the presence of phosphorus indicates an enhancement of Mo proportion in an oxide environment or coordinatively unsaturated sites (anionic vacancy). These results are in agreement with XPS analysis, which showed an increase of proportion of $Mo^{4+}$ and $Mo^{6+}$ in P-doped catalysts (Table 5).

For the Ni-containing catalyst, the pyridine spectrum presented a shoulder at around 1608 $cm^{-1}$ of similar intensity to that of the sample without Ni (not shown) indicating that Ni-containing carbide is less acidic than P-doped carbide.

Results of pyridine adsorption for non-promoted and P-doped carbide catalysts supported on alumina showed that intensity of 1608 $cm^{-1}$ band, characteristic of coordination sites, increased with the amount of P. Addition of P increased the number of Lewis sites in the carbide phase and enhanced the $Mo^{4+}$ abundance, as observed by XPS analysis (Table 5). The peak area of 1608 $cm^{-1}$ band was linearly correlated with the abundance of $Mo^{4+}$ oxidation state given by XPS analysis (Fig. 6a).

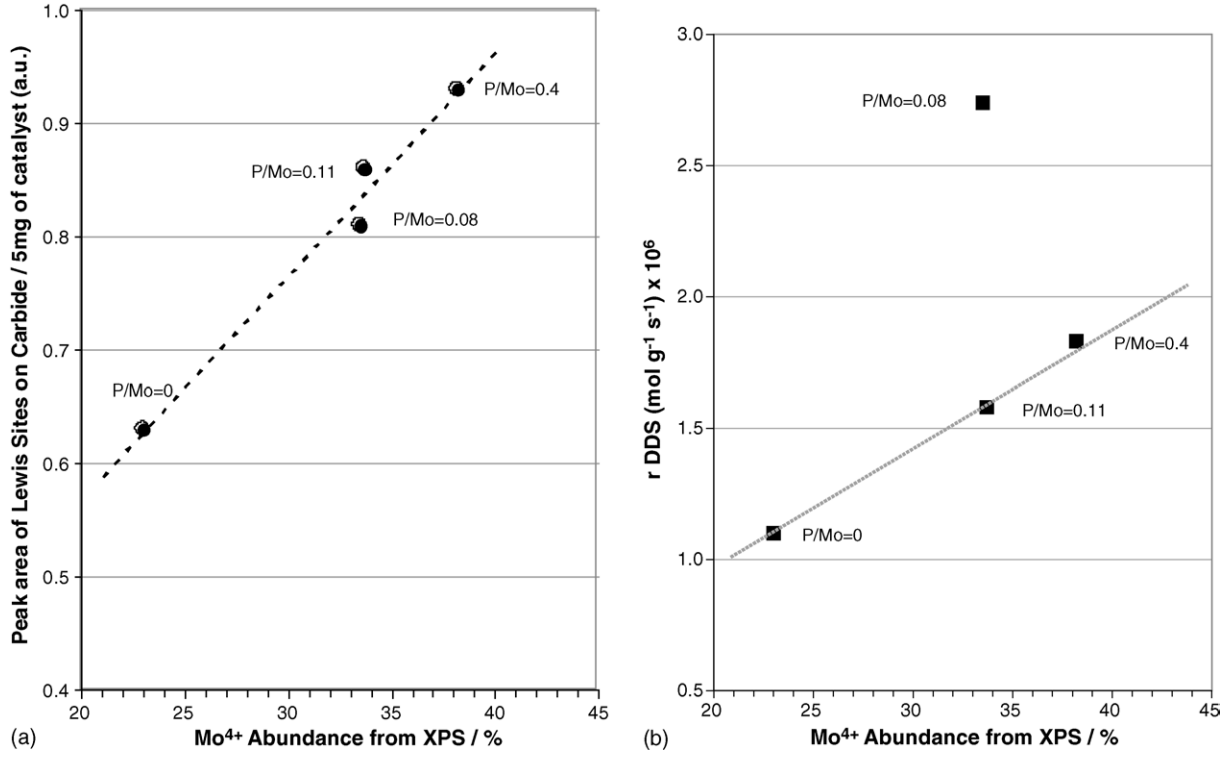


Fig. 6. (a) Relationship between peak area at 1608 $cm^{-1}$ (pyridine IR spectra) and $Mo^{4+}$ abundance from XPS spectra of alumina-supported molybdenum carbides; (b) relationship between DDS rate and $Mo^{4+}$ abundance from XPS spectra of alumina-supported molybdenum carbides.

When the DDS rate was plotted against the $Mo^{4+}$ abundance (Fig. 6b), only the $Mo_2CP(0.08)$ catalyst did not correlate, indicating that $Mo^{4+}$ were active centers for 4,6-DMDBT hydrodesulfurization only in alumina-supported molybdenum carbides.

On the contrary, for Ni-promoted catalysts, no correlation was observed. The $Mo^{4+}$ abundance, which was related to the DDS pathway for the P-promoted carbide, was only 25% of the total molybdenum abundance. The IR-pyridine spectrum also presented a shoulder at around 1608 $cm^{-1}$ but its intensity was similar to that of the non-promoted catalyst.

The $Mo^{\delta+}$ abundance in Ni-promoted catalysts was lower than that of a non-promoted catalyst but higher than for P-containing materials. However, the NiMoC/Al catalyst gave the highest overall and DDS rates for 4,6-DMDBT HDS. Therefore, active sites involved in P-promoted alumina-supported molybdenum carbides did not allow us to explain the high activity of Ni-promoted catalysts. FT-IR experiments of adsorbed CO [8] revealed synergetic effects resulting from complex chemical combinations of Ni and molybdenum carbides on alumina as those observed for NiMoS/Al. So, ''Ni–Mo–C'' entities could also be considered as active sites in this case but more studies are needed. Lewis acid sites from cardidic phases are the most active species for HDS of 4,6-DMDBT.

We proposed a mechanism based on that of Bataille et al. [18] for C–S bond cleavage of 4,6-DMDBT. The first step (HYD step) is the double bond hydrogenation in the vicinity of sulfur atom. The second step (for the DDS pathway) is the C–S bond opening by an elimination process, involving an attack of a hydrogen atom by a carbon of the supported molybdenum carbide acting as a basic site; the hydrogen atom being in the β-position relative to the sulfur atom. According with this mechanism, the main effect of phosphorus is presumably the increase of basicity of carbon atoms in carbide.

### *3.4. Reactivity of promoted alumina-supported molybdenum carbides in real feedstocks conditions*

Different alumina-supported molybdenum carbides catalysts were compared to a commercial $CoMoS/Al_2O_3$ catalyst during HDS of real feedstocks (GO1, 520 wt. ppm S). After 20 h of time on stream, at 613 K under 3 MPa total pressure, the sulfided catalyst is the most active catalyst. For GO2 (135 wt. ppm S), the results were different (Table 6); at 613 K, the HDS conversion with $Mo_2CP(0.11)/Al$ was 41% whereas with CoMoS/Al the conversion was about 56%. Although the supported carbide with P/Mo = 0.11 ratio presented higher conversion (41%) than the material with P/Mo = 0.4 (24%), this latter catalyst was more efficient to reduced the refractory sulfur compounds. Indeed, the 4,6-DMDBT was significantly reduced with $Mo_2CP(0.4)/Al$. Neither sulfided commercial catalyst, nor promoted or non-promoted alumina-supported molybdenum carbide catalysts transformed efficiently C2-dibenzothiophene under these operating conditions (3 MPa, 613 K).

For both gas oil studies, only $Mo_2CP(0.4)/Al$ catalyst was active for the hydrogenation of aromatics (HDA). For the HDS of GO1, the distribution of aromatics compounds was modified, from 23% monocyclic, 5.4% dicyclic and 1.3% polycyclic in the feed to 22.6% monocyclic, 6.3% dicyclic and 0.1% polycyclic in the products. Such results indicate that polycyclic and monocyclic compounds were converted preferentially. On the contrary, during the HDS of GO2, the dicyclic and polycyclic were hydrogenated. For other catalysts (commercial sulfide, $Mo_2CP(0)/Al$ and $Mo_2CP(0.11)/Al$) dehydrogenation was observed. Hydrogenation of two deep hydrotreated gas oils (0.5 wt. ppm S (GO3) and 47 wt. ppm S (GO4)) were followed by HPLC after 20 h of time on stream and after reaching the steady state. In these operating conditions, $Mo_2CP(0.4)/Al$ which has been previously found as the most hydrogenating catalyst, was not active. However, the bulk ($Mo_2CEM$) and the alumina supported Ni-doped catalyst (NiMoC/Al) were as active as a commercial sulfided catalyst (NiMoS/Al (HR348)). For the HDS using GO1 and GO2, the same conclusions can be reached for $Mo_2CP(0.4)/Al$. However, both $Mo_2CEM$ and NiMoC/Al were more hydrogenating catalysts than HR348.

During experiments with GO4 and GO3, the total sulfur and nitrogen contents were followed by fluorescence X using a X-MET 920 (Metorex) analyzer. For GO4 (Fig. 7a), all carbide catalysts (supported or bulk) possessed higher

Table 6
Sulfur detection (wt. ppm) in studied gas oils after catalyst stabilisation, total pressure 30 bar and $T = 613$ K, GO2 (135 wt. ppm S), running time, 36 h

| Sulfur compound | Feed | $Mo_2CP(0.11)/Al$ | $Mo_2CP(0.4)/Al$ | CoMoS/Al |
|---|---|---|---|---|
| Dibenzothiophene | 1 | 0 | 0 | 0 |
| C1 dibenzothiophene | 14 | 0 | 6 | 0 |
| C2 dibenzothiophene | 31 | 27 | 26 | 25 |
| 4.6 DMDBT | 19 | 18 | 15 | 19 |
| C3 dibenzothiophene | 29 | 27 | 27 | 20 |
| C3+ dibenzothiophene | 60 | 22 | 43 | 15 |
| Total sulfur | 135 | 80 | 102 | 60 |
| HDS conversion (%) | | 40.8 | 24.4 | 55.5 |

C1 dibenzothiophene, one C bond with dibenzothiophene; C2 dibenzothiophene, two C bonds with dibenzothiophene; C3 dibenzothiophene, three C bonds with dibenzothiophene; C3+ dibenzothiophene, more than three bonds with dibenzothiophene.

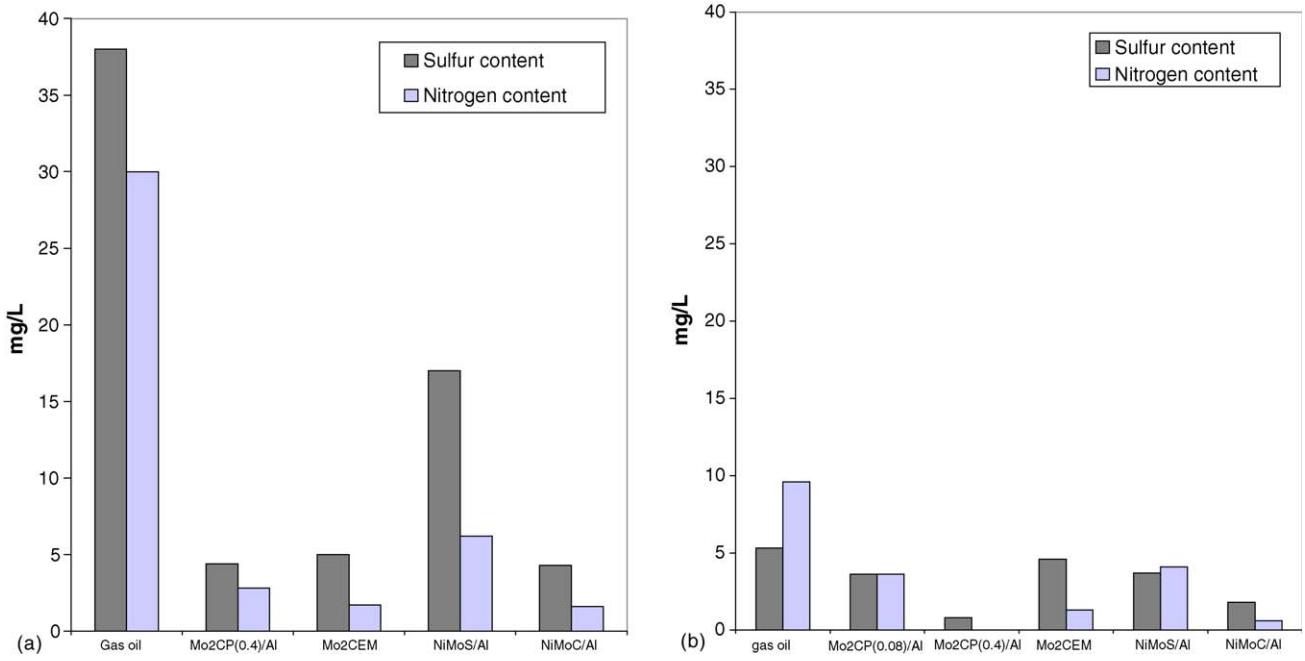


Fig. 7. Sulfur and nitrogen content (mg/L) in the feed and in the hydrotreated gas oils after 20 h of run at 613 K for the gas oils: (a) containing 47 ppm S; (b) containing 0.05 wt. ppm S.

HDN and HDS activities than the commercial sulfide catalyst. At these sulfur and nitrogen levels (0–50 ppm), only the most refractory compounds remained in the feed [21,22]. In this case, the ranking of global hydrodesulfurization rate was: NiMoS/Al $\ll$ $Mo_2CEM$ < $Mo_2CP(0.4)$/Al < NiMoC/Al; while the ranking of global HDN was: NiMoS/Al < $Mo_2CP(0.4)$/Al < $Mo_2CEM$ < NiMoC/Al.

For GO3 (Fig. 7b), results were close to previous but the ranking of catalysts was modified. The ranking of global HDS activity was: $Mo_2CEM$ < NiMoS/Al $\sim$ $Mo_2CP(0.08)$/Al < NiMoC/Al < $Mo_2CP(0.4)$/Al; while the ranking of global hydrodenitrogenation was: NiMoS/Al $\sim$ $Mo_2CP(0.08)$/Al < $Mo_2CEM$ < NiMoC/Al < $Mo_2CP(0.4)$/Al. For these latter experiments using hydrotreated feedstocks, the catalysts (NiMoC/Al and $Mo_2CEM$) possessing a higher activity in HDA were also very active in deep HDN and HDS.

## 4. Conclusions

Deep HDS of 4,6-DMDBT was performed on selected promoted alumina-supported molybdenum carbides. Ni or P increased significantly the HDS rate in laboratory scale experiments.

The total conversions (HDS, HDA) in industrial conditions (GO1 (520 wt. ppm S)) indicated that alumina supported molybdenum carbides were not as active as a commercial catalyst (CoMoS/Al) in HDS. However, P-doped catalysts, such as $Mo_2CP(0.4)$/Al were more active in HDA than the commercial one.

These results also indicated that phosphorus promoted alumina supported carbide catalysts were as active as a commercial Co–Mo/$Al_2O_3$ catalyst for low levels of sulfur in the feed (lower than 135 wt. ppm). Furthermore, refractory compounds such as 4,6-DMDBT were transformed only on molybdenum carbide catalyst under industrial conditions for hydrotreated gas oils, indicating a good performance in HDS of refractory compounds.

For deep hydrotreated gas oils (<47 wt. ppm S), the phosphorus promoted molybdenum carbide catalysts became more active than commercial catalyst (HR346C) for HDA and HDS or HDN of the feedstock. However, alumina supported Ni-doped molybdenum carbides or bulk carbides were more active than P-doped materials in these latter reactions.

The sulphur-tolerant catalysts: $Mo_2CP(0.4)$/Al < $Mo_2CEM$ < NiMoC/Al could substitute noble metal or sulfided catalysts for deep HDS of gas oil fuels or HDA of feedstocks with very low level of sulfur.

## Acknowledgements

This work was carried out in the framework of the program ‘‘Post-traitement des coupes gazoles hydrotraitées’’. The authors thank IFP, TOTAL, PROCATALYSE and CNRS-Ecodev for supporting this work.

## References

[1] T. Kabe, A. Ishihara, H. Tajima, Ind. Eng. Chem. Res. 31 (1992) 218.
[2] A. Ishihara, H. Tajima, T. Kabe, Chem. Lett. (1992) 669.
[3] X. Ma, K. Sakanishi, T. Isoda, I. Mochida, Ind. Eng. Chem. Res. 34 (1995) 748.

[4] D.D. Whitehurst, T. Isoda, I. Mochida, Adv. Catal. 42 (1998) 345.
[5] M.V. Landau, Catal. Today 36 (1997) 393.
[6] H.K. Park, D.S. Kim, K.L. Kim, Kor. J. Chem. Eng. 15 (1998) 625.
[7] P. Da Costa, C. Potvin, J.-M. Manoli, J.-L. Lemberton, G. Perot, G. Djega-Mariadassou, J. Mol. Catal. A 184 (2002) 323.
[8] J.-M. Manoli, P. Da Costa, F. Mauge, M. Brun, M. Vrinat, C. Potvin, J. Catal. 221 (2004) 365.
[9] D.J. Sajkowski, S.T. Oyama, Appl. Catal. A 134 (1996) 339.
[10] D.J. Sajkowski, S.T. Oyama, US Patent 5,200,060 (1993) to Amoco Corporation.
[11] P. Da Costa, J.-M. Manoli, C. Potvin, G. Djega-Mariadassou, P. Da Silva, S. Kasztelan, F. Diehl, M. Breysse, US Patent 6,372,125 (2001) to Institut Francais du Petrole.
[12] P. Da Costa, J.-L. Lemberton, C. Potvin, J.-M. Manoli, G. Pérot, M. Breysse, G. Djéga-Mariadassou, Catal. Today 65 (2001) 195.
[13] R.A. Burdett, L.W. Taylor, L.C. Jones Jr., Molecular Spectroscopy, vol. 38, The institute of Petroleum, 1955.
[14] P.A. Aegerter, W.W.C. Quigley, G.J. Simpson, D.D. Ziegler, J.W. Logan, K.R. McCrea, S. Glazier, M.E. Bussell, J. Catal. 164 (1996) 109.
[15] J.S. Lee, K.H. Lee, J.Y. Lee, J. Phys. Chem. 96 (1992) 362.
[16] B. Dhandapani, S. Ramanathan, C.C. Yu, B. Frühberger, J.G. Chen, S.T. Oyama, J. Catal. 176 (1998) 61.
[17] P. Perez-Romo, C. Potvin, J.-M. Manoli, M.M. Chehimi, G. Djéga-Mariadassou, J. Catal. 208 (2002) 187.
[18] F. Bataille, J.-L. Lemberton, P. Michaud, G. Pérot, M. Vrinat, M. Lemaire, E. Schulz, M. Breysse, S. Kasztelan, J. Catal. 191 (2000) 409.
[19] K.T. Ng, D.M. Hercules, J. Phys. Chem. 80 (1976) 2094.
[20] C. Lahousse, A. Aboulayt, F. Maugé, J. Bachelier, J.-C. Lavalley, J. Mol. Catal. 84 (1993) 283.
[21] A. Amorelli, Y.D. Amos, C.P. Halsig, J.J. Kosman, R.J. Jonker, M. De Wind, J. Vrieling, Hydrocarb. Process. (1992) 93.
[22] H. Schulz, W. Böhringer, F. Ousmanov, P. Waller, Fuel Process. Technol. 61 (1999) 5.